Hindawi
Geofluids
Volume 2021, Article ID 9740302, 13 pages
https://doi.org/10.1155/2021/9740302

Research Article

Study on the Creep Damage Characteristics of Shale under the Combined Action of Osmotic Pressure and Disturbance Load

Junguang Wang, Qingrong Yu, Bing Liang, and Zhangqing Xuan

Institute of Mechanics and Engineering, Liaoning Technical University, Fuxin 123000, China

Correspondence should be addressed to Junguang Wang; shenliu_303@126.com

Received 2 October 2021; Accepted 5 November 2021; Published 20 November 2021

Academic Editor: Yanan Gao

In the in situ modified fluidized mining engineering, the surrounding rock of the shaft wall is prone to creep instability damage under the action of disturbance and seepage water pressure, which seriously affects the stability of the surrounding rock of the deep in situ modified fluidized mining. In order to study the nonlinear creep damage and fracture characteristics of deep rocks under the combined action of seepage water pressure and disturbance load, a self-developed rock perturbation creep test rig under the action of seepage water pressure was used, and shale was used as the rock sample. In the method of staged loading, the rock uniaxial compression perturbation creep test under static axial pressure, different perturbation frequencies, and different seepage water pressures was carried out, and the creep characteristics of shale under the combined action of perturbation and seepage were studied. The results show that with the increase of seepage water pressure, the creep failure time of the rock decreases, and the ultimate strain value increases; with the increase of the disturbance frequency, the creep failure mode of the rock gradually transitions from shear failure to tension failure. When water pressure and disturbance load exist at the same time, rock creep is more sensitive to seepage water pressure; based on experimental results, a shale perturbation creep damage model considering the influence of seepage water pressure and disturbance frequency is established, and the model is verified. The research results have important theoretical significance for guiding the wellbore stability control of in situ modified fluidized mining engineering.

1. Introduction

The in situ modified fluidized mining method is accompanied by the development of new and unconventional geological resources such as hot dry rock geothermal, oil shale, and coalbed methane, which are difficult to be effectively mined by traditional methods. Its engineering first needs drilling on the surface to form a mining well pattern and then use these well patterns to connect the fracture network along the bedding and finally implement the in situ modified fluidized mining project of minerals at low cost and efficiently. However, the walls of these mining well patterns are affected by water seepage pressure and drilling disturbances in the deep space, and the well walls are subject to creep behavior under high ground stress conditions at all times, which has a great impact on the stability of the well walls, or even interrupts in situ modified fluidized mining engineering.

At present, for the research of rock damage and rheology, experts at home and abroad have carried out detailed rock creep tests under different seepage effects, the same pore water pressure, and different water-bearing conditions and have established a creep constitutive considering water content. Relational theory, discussing the influence of water content on the creep characteristics of rocks, has yielded fruitful research results. Xiaozhao et al. [1] obtained a macro-meso-mechanical model of the stress-strain constitutive relationship of brittle rock under the action of osmotic pressure-driven crack propagation through theoretical derivation and experimental verification. Wu et al. [2] established the creep constitutive equation of the combined action of water pressure and external force and gave a method to solve the model parameters. Wang et al. [3] used the differential equation description method to discuss the change law of model parameters

and the corresponding stability during the creep damage process. Junguang et al., Chen et al., and Yajun et al. [4–7] studied the mechanical properties of rock creep under the action of water and obtained fruitful research results. Zhiliang, Gao et al., Wang et al., and Cui et al. [8–11] studied the creep mechanical properties of rock under disturbance and obtained the influence of disturbance on rock creep. Su et al. [12] studied the influence of periodic disturbance on rock mechanical properties. Jianguo and Zhu and Qi-Hu et al. [13, 14] introduced damage variables from different angles and established a rock damage creep model. M'Barki et al. [15] studied the influence of rock composition and microstructure on the rheology of steam foam in sandstone reservoirs. Souley et al. [16] conducted in situ measurement of granite permeability and numerical simulation of permeability changes caused by microcrack propagation. Boukharov et al. [17] studied the three basic processes (elasticity, plastic, and expansion deformation) in brittle rock under continuous load, proposed a creep model adapted to brittle rock, and developed an analytical creep curve for estimating the method of basic parameters of rock creep. However, with the increase of mining depth, the influence of engineering disturbance and seepage water pressure on rock creep damage is more significant, and engineering disturbance and seepage water pressure directly affect the creep damage and rupture law of rock.

The academic research on the law of rock creep under the coupling action of disturbance and seepage is not perfect, and there are few related researches. The thesis takes shale as the research object and conducts rock creep damage experiments under different seepage water pressures and different disturbance conditions to study the response of multiple factors to the rock creep law from a macro- and mesoscopic perspective to explore the seepage pressure and disturbance. This has important theoretical guiding significance for the wellbore stability control of in situ modified fluidized mining engineering.

2. Uniaxial Disturbance Creep Experiment of Shale under Osmotic Pressure

2.1. Test Equipment. The test equipment adopts the self-made rock seepage-disturbance-creep test bench of Liaoning Technical University. The test rig consists of 6 parts in total, which are three-axis pressure chamber, frequency modulation system, effective stress loading system, hydraulic loading system, data monitoring system, and disturbance loading system, as shown in Figure 1.

2.1.1. Axial Load System. Axial pressure loading is mainly realized by the principle of lever. The lever arm ratio is changed by adjusting the position of the movable support, and the amount of applied axial pressure is changed by the weight of the weight on the weight table.

2.1.2. Disturbance and Seepage Loading System. The disturbance loading is mainly realized by the YZU-30-6B vibration motor at the upper right end of the rigid beam A. By changing the angle between the eccentric blocks on the main shafts at both ends of the motor, an exciting force of 5-20 kN can be generated to achieve loading of different disturbance amplitudes. Link the motor with the SRMCO-VM05 inverter, and by changing the inverter frequency, different loading frequency disturbance loads can be applied, usually within the range of 0-10 Hz. The osmotic water pressure loading is mainly realized by a water pump. The water pump is used to squeeze the water into the seepage channel above the rock specimen, and the magnitude of the applied osmotic water pressure can be obtained by observing the value of the pressure gauge A.

2.1.3. Data Monitoring System. Data collection is mainly realized by TOPRIE data logger. Connect the pressure sensor to the TOPRIE data recorder, and monitor the changes in stress and displacement during the experiment through the change of the indication on the recorder. Connect the DHDAS collector to the rock and the computer to obtain the rock strain during the test.

2.2. Test Plan and Process. The test rock sample was taken from the 12th Pingmei Coal Mine. The sampling depth is 759 m shale. The selected shale is gray-black laminar shale with gray-white bioclastic sedimentary microlayers and siltstone layers. The rock has thin page shaped or lamellar joints. In order to ensure the comparability of the samples, the sample layers and locations are the same. According to the requirements of the experimental equipment for the size of the specimen, a cylindrical shale specimen of Φ50 mm × 100 mm was prepared. The nonparallelism of the two ends of the rock sample is less than 0.05 mm, and the processing accuracy meets the requirements of the regulations. Using ultrasonic testing, select the specimens close to the sound speed and sound time, and test the rock samples with good consistency. The number of specimens is 6 pieces. The experimental parameters set for each test piece are shown in Table 1. The average uniaxial compressive strength of shale is 63.5 MPa. Considering that the influencing factors of rock creep failure are disturbance load frequency and seepage water pressure, the disturbance amplitude is selected to be 3.2 MPa; the disturbance frequency is 3 Hz, 6 Hz, and 9 Hz; and the seepage water pressure is 3 MPa, 5 MPa, and 7 MPa to roughly simulate the stress environment of the well wall.

The specific test process is as follows:

(1) Connect the strain gauge. Before the experiment, paste the prepared BX120-20AA strain gauge to the rock surface through glue, and connect the other end to the DHDAS collector through a wire to monitor the amount of strain during the experiment

(2) Install the test piece. Fix the prepared rock test piece in the middle of the upper and lower pressure heads, seal the test piece around with a heat shrinkable film, seal the test piece in the triaxial pressure chamber on the base of the creep test bench, and check the air tightness of the device

(3) Apply axial pressure. Place the predetermined number of weights on the weight table to obtain the predetermined axial pressure

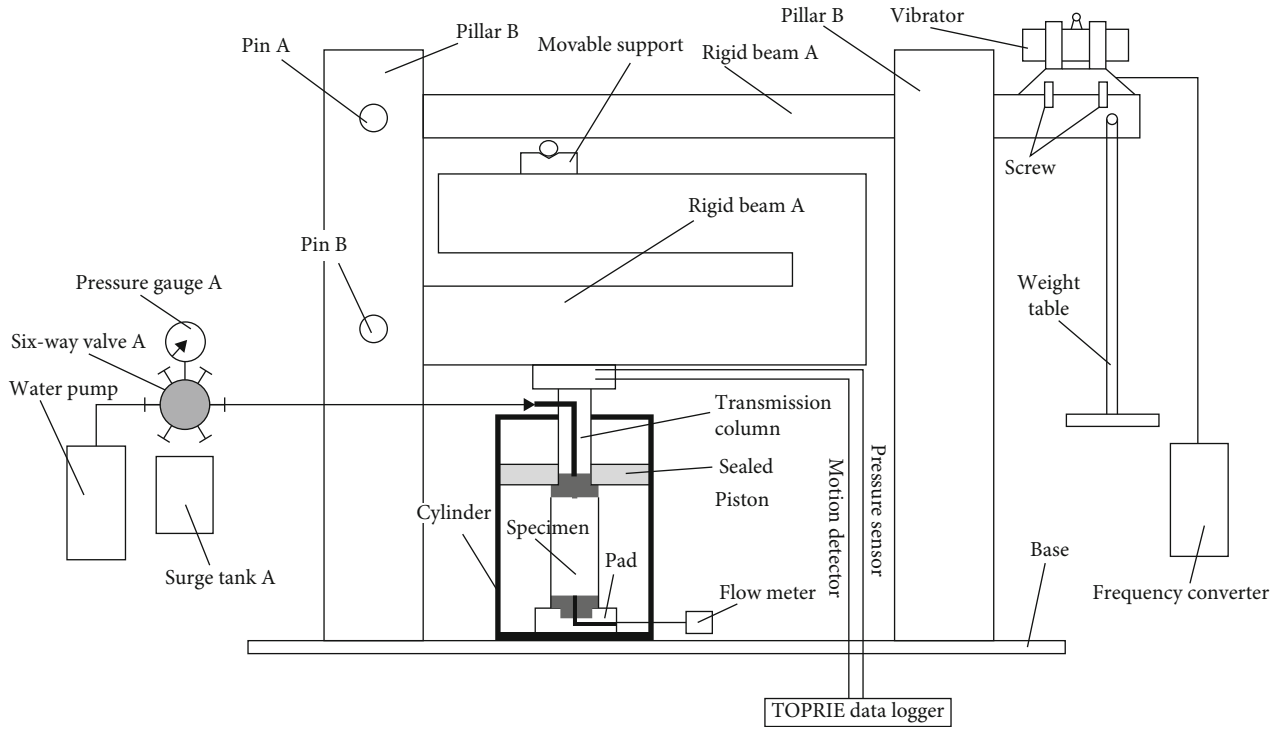

Figure 1: Percolation-perturbation creep test bed.

Table 1: Test scheme.

Influencing factors	Specimen number	Axial pressure σ/MPa	Disturbance frequency p_iHZ	Osmotic pressure/MPa
Axial pressure	D1	15, 25, 35, 45, 55	—	—
Osmotic pressure	D2	15, 25, 35, 45, 55	6	3
	D3	15, 25, 35, 45, 55	6	5
	D4	15, 25, 35, 45, 55	6	7
Disturbance load frequency	D5	15, 25, 35, 45, 55	3	5
	D6	15, 25, 35, 45, 55	9	5

When the first axial pressure "15 MPa" was loaded, the rest axial pressures are loaded with waiting a period one by one.

(4) Apply osmotic water pressure. Turn on the water pump, six-way valve A, pressure gauge A, and surge tank A; apply the permeating water pressure to the specified value at a rate of 0.05 MPa/s, and keep the water pressure constant

(5) In order to simulate the impact of drilling disturbance on the fluidized mining shaft wall, a YZU-30-6B vibration motor was used to apply disturbance load in the axial direction of the specimen. The applied disturbance load waveform is a sine curve, which is adjusted to the required disturbance frequency value by the SRMCO-VM05 inverter. The disturbance load is shown in Figure 2. When doing different seepage water pressure tests, turn off the vibrating motor after 6 hours and increase the axial pressure by 10 MPa. Repeat this step until the test piece is damaged. After the test, the test piece is taken out. When doing different disturbance frequency tests, turn off the vibrating motor when the strain reaches a certain value, increase the axial pressure by 10 MPa, and repeat the above steps

2.3. Test Results and Analysis

2.3.1. Overall Analysis of Creep Curve

(1) Analyzing all the shale creep curves in Figure 3 shows that when the axial pressure is low, the shale creep rate tends to be stable, but it increases as the axial pressure increases. When the load continues to increase, the amount of shale deformation gradually increases within the same time. When the load increases further, the shale enters the accelerated creep stage; that is, the amount of deformation increases sharply in a short time

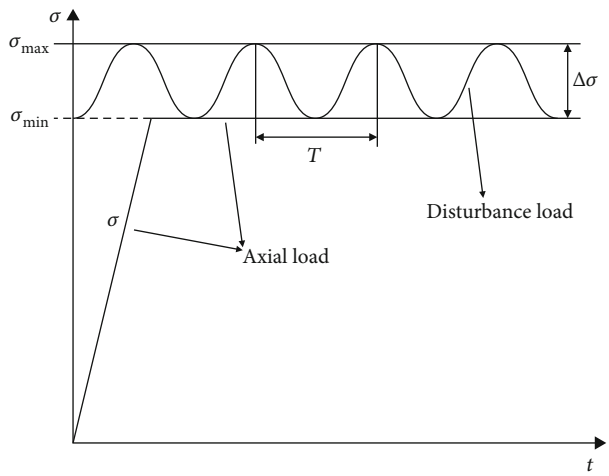

Figure 2: Schematic diagram of disturbance load.

(2) Comparing Figure 3(a) with Figures 3(b)–3(f), we can see that regardless of the axial pressure, the creep deformation of shale is greater when there is disturbance than when there is no disturbance. When the rock is completely broken, the axial pressure is greater when there is no disturbance than when there is disturbance, and the time for the rock to creep and rupture is the longest when there is no disturbance. When a disturbance load is applied, the creep rupture speed of the rock increases, and the axial stress value when the rock is completely ruptured slightly decreases

(3) As shown in Figures 3(b) and 3(c), during the creep process, the amount of rock creep deformation increases with the increase of seepage water pressure. The increase in axial pressure results in the further development of internal fractures in the rock, resulting in an increase in the space for water penetration. When the seepage water pressure is increased, the inner pore walls of the rock are affected by the seepage water pressure, which leads to plastic failure inside the rock and further opens up the cracks inside the rock. Therefore, the amount of creep deformation of the rock increases

(4) As shown in Figure 3(d), when the seepage pressure is 7 MPa, the axial stress required for the rock to enter the accelerated creep stage is 35 MPa. As shown in Figure 3(f), when the disturbance frequency is 9 Hz, the axial stress required for the rock to enter the accelerated creep stage is 45 MPa. As shown in Figure 3(a), when there is no perturbation load and no seepage water pressure, the axial stress required for the rock to enter the accelerated creep stage is 55 MPa. This shows that both the disturbance load and the seepage pressure affect the strength of the rock. With the increase of seepage pressure and frequency of disturbance, the degree of damage inside the rock also increases, and the strength of the rock decreases

As shown in Figure 3(a), under undisturbed conditions, the total time from load application to complete creep failure of shale (hereinafter referred to as shale creep failure time) is 1550 min, and the total axial strain of shale is 1.939%. As shown in Figures 3(e), 3(c), and 3(f), the disturbance frequencies are 3 Hz, 6 Hz, and 9 Hz, respectively; the creep failure time of shale is 1359.3 min, 1285.9 min, and 1288.7 min; and the total strain of shale is 2.041%, 2.110%, and 2.229%, respectively. As the seepage pressure increases, the shale creep failure time is significantly reduced. The perturbation frequency has little effect on the shale creep failure time, and the total strain also increases slightly with the increase of the perturbation frequency. The total creep deformation of shale is more affected by perturbation than osmotic pressure.

2.3.2. Analysis of Shale Macroscopic Fracture Pattern

(1) Analysis of Creep Macrofailure Mode under Undisturbed and Disturbed Conditions. It can be seen from Figure 4 that under the same axial pressure, the applied disturbance load affects the macroscopic creep failure mode of shale. Under the condition of no disturbance load, the shale failure mode is relatively simple. The macroscopic creep failure mode of the specimen is shear failure. The specimen has only one obliquely penetrating main crack with an axial angle of about 25°. The main crack divides the specimen into two parts of equal size. Under the effect of disturbance, the macroscopic creep failure mode of shale is very complicated, and multiple failure modes coexist. Compared with the effect of disturbance, the number of shale microcracks increases, and the degree of shale creep damage is obviously enhanced.

(2) Analysis of Creep Macroscopic Failure Mode under Different Perturbation Frequency. Figure 4(e) shows the macroscopic creep failure diagram of the rock under the disturbance frequency $f = 3$ Hz. The analysis shows that the test piece is divided into two parts along the diagonal. At the same time, a new crack was derived from the middle position of the rock bottom, and the new crack gradually penetrated upwards, finally forming a secondary tension crack, but no penetration surface appeared. Because the upper and lower surfaces of the rock block are not flat enough, there is an inclination angle between the lower end of the rock and the pressure table, so the stress of the shale is uneven, and the damage of the left half of the shale is more serious. Figure 4(f) is the macroscopic creep failure diagram of the rock under the disturbance frequency $f = 9$ Hz. It can be seen that the number of cracks in the rock increases, and the rock failure mode is more complicated. There are obviously two through cracks on the rock surface: one is perpendicular to the horizontal plane on the right side of the rock, which is a tensile crack, and the other is a shear crack at an angle of 60° with the horizontal plane. The second shear crack has a greater degree of damage, and two tiny secondary tension cracks are gradually derived from this crack. This shows that as the frequency of disturbance increases, the tensile failure accompanying rock shear failure increases. This is because the internal microcracks of shale cyclically open and close under

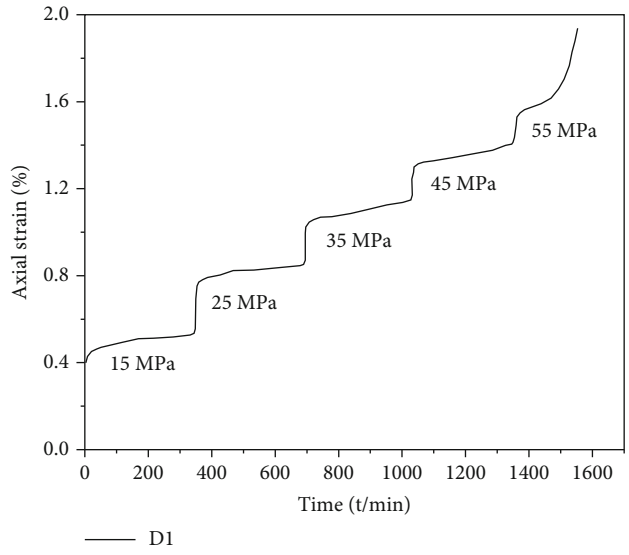

(a) No disturbance, no water pressure

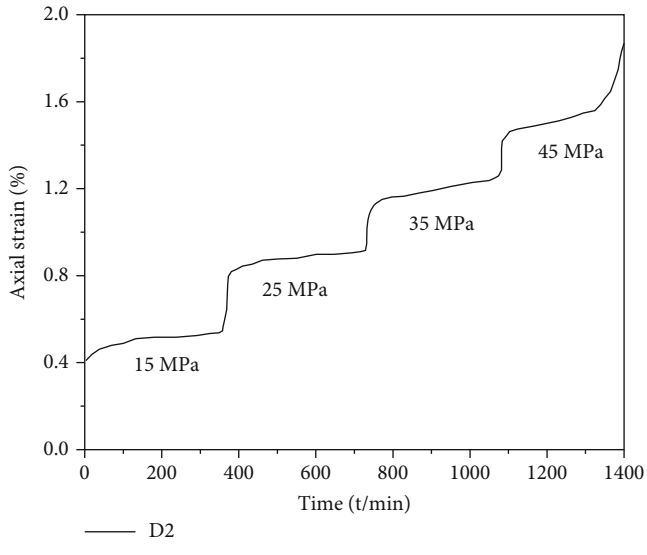

(b) $f = 6$ Hz, $p = 3$ MPa

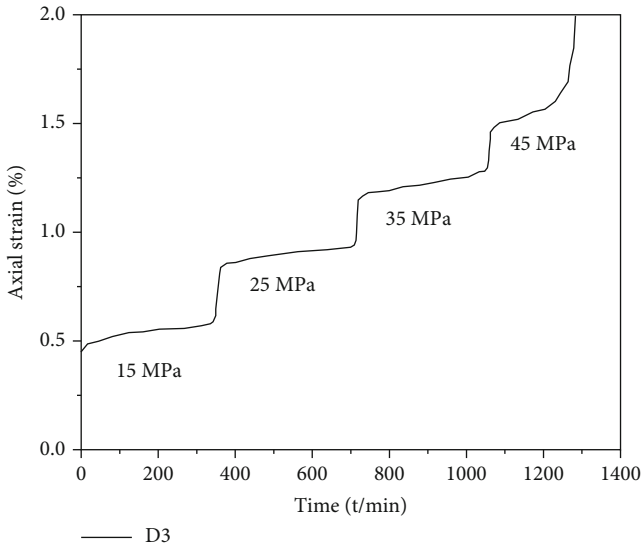

(c) $f = 6$ Hz, $p = 5$ MPa

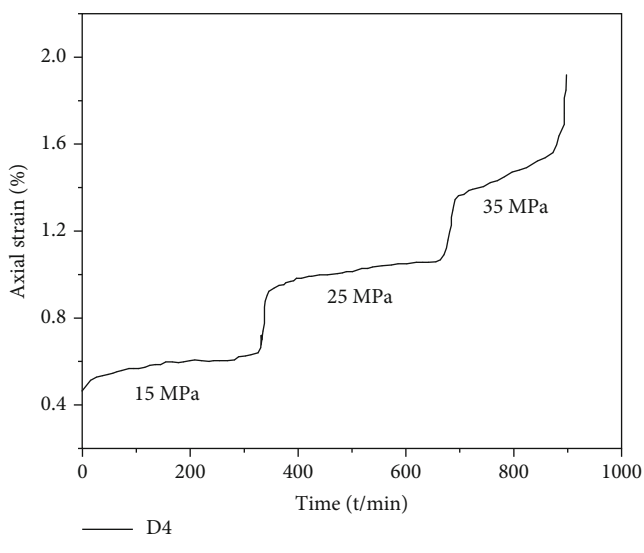

(d) $f = 6$ Hz, $p = 7$ MPa

Figure 3: Continued.

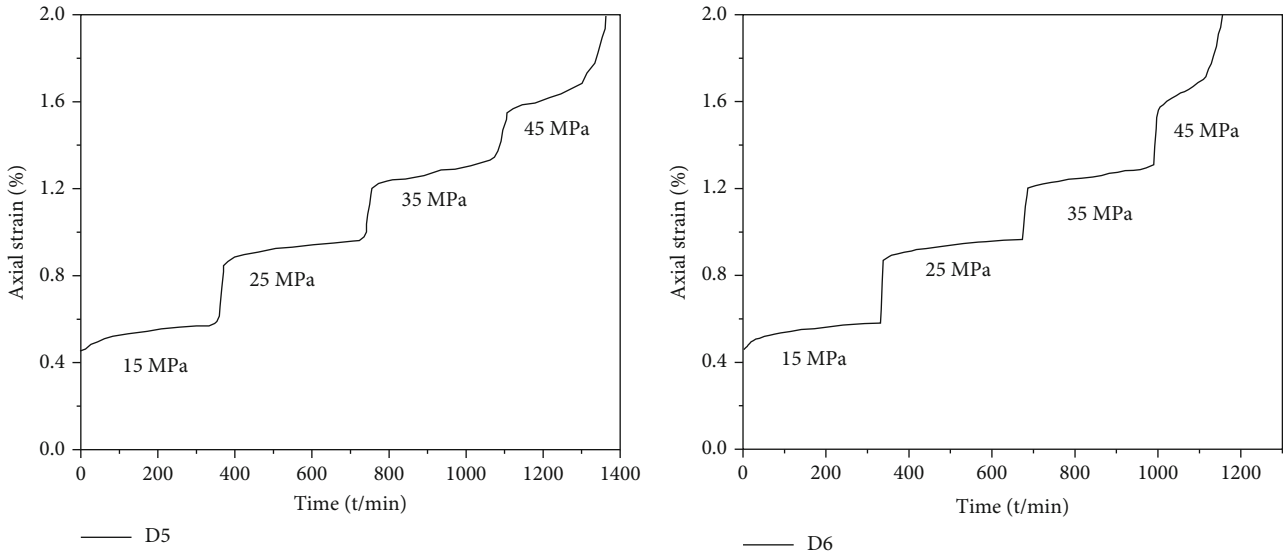

Figure 3: Rock disturbance creep curves.

disturbance conditions, and the rock is more prone to tensile cracks. As the frequency of disturbance increases, this situation will become more serious.

(3) Analysis of Macroscopic Failure Mode of Disturbance Creep under Osmotic Water Pressure. Under the condition of disturbing load, the pressure of seepage water is applied, and the macroscopic creep failure mode of rock becomes more complicated. When the seepage water pressure is 3 MPa, there is a major crack on the surface of the rock after failure, which is a shear failure crack that penetrates from the upper right of the rock to the lower left of the rock. Compared with the nonpermeable water pressure, there are three more fractures on the rock surface: one secondary shear fracture parallel to the main crack, one secondary tension fracture connecting the upper end of the rock and the main fracture, and one connecting the main fracture and the secondary shear cut the secondary tension crack of the fissure. The rock failure mode is mainly shear failure and local tension failure. At the same time, the disturbance load causes uneven contact between the lower end of the rock and the plane of the pressure table, and the edge breaks off. When the seepage pressure increases to 5 MPa, the rock failure mode is still dominated by shear failure. In addition to a shear crack similar to the main crack when the seepage pressure is 3 MPa, there is another shear crack on the right side of the rock that penetrates the upper and lower surfaces of the rock. At the same time, two secondary tension cracks extending downward are derived from the middle of the main crack. Compared to when the osmotic water pressure is 3 MPa, the shear failure degree when the osmotic water pressure is 5 MPa is more serious. When the seepage water pressure is increased to 7 MPa, the rock surface is penetrated by three tension cracks. Due to the small inclination of the three tension cracks, the rock was divided into three parts of different sizes, and a downward shear crack was derived in the middle of the specimen. The entire rock is relatively complete, with a slight shedding at the lower right end.

In summary, when the perturbation frequency is constant, as the seepage pressure increases, the degree of rock macroscopic damage increases. When the water seepage pressure is low, the damage degree of the rock is relatively low, and the rock is more complete after the damage. With the increase of osmotic water pressure, the failure mode of rock transitions from the failure of tension-shearing to the failure dominated by tension, and the number and length of tension cracks in the rock increase. The number and length of tensile cracks produced by the rock increase. With the increase of seepage pressure, the macroscopic damage degree of the rock under the perturbation creep increases, and the sensitivity of the rock damage to the perturbation also increases.

3. Research on Damage and Creep Model of Shale under Osmotic Pressure

3.1. Establishment of Damage Variables. It can be seen from the test results that the creep characteristics of shale are related to axial pressure, axial pressure disturbance frequency, and seepage water pressure and time. When the load gradually increases or the load acts for a long time, new microcracks will sprout in the initial voids inside the rock. As the creep time goes by, more and more fine cracks will be produced. When the number of tiny cracks accumulates to a certain extent, they will accelerate and expand at a nonlinear speed until the rock finally breaks. In order to establish a shale perturbation creep damage model, this paper introduces the damage variable D according to the Kachanov creep damage theory [18]. The damage variable D is a

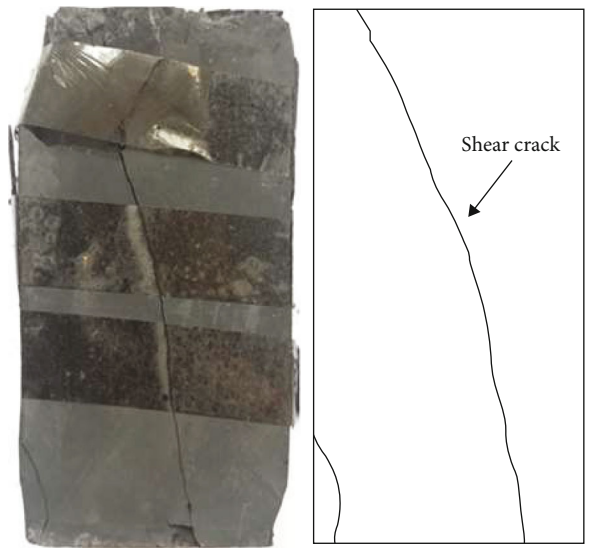

(a) No disturbance, no water pressure

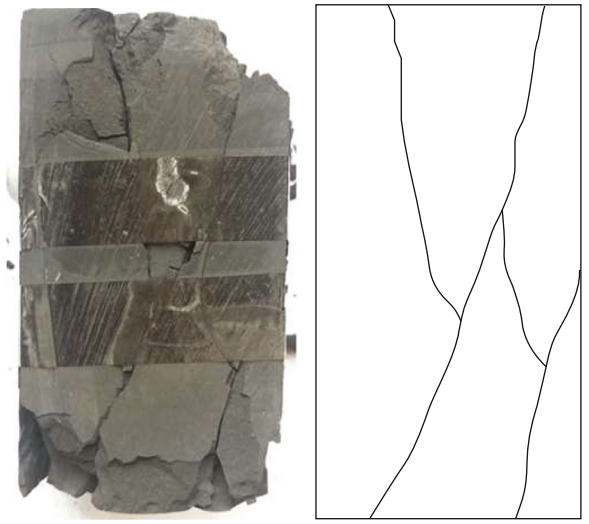

(b) $f = 6$ Hz, $p = 3$ MPa

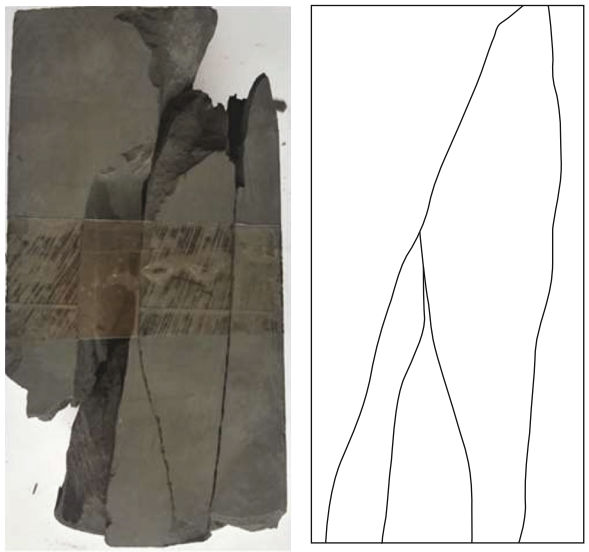

(c) $f = 6$ Hz, $p = 5$ MPa

(d) $f = 6$ Hz, $p = 7$ MPa

Figure 4: Continued.

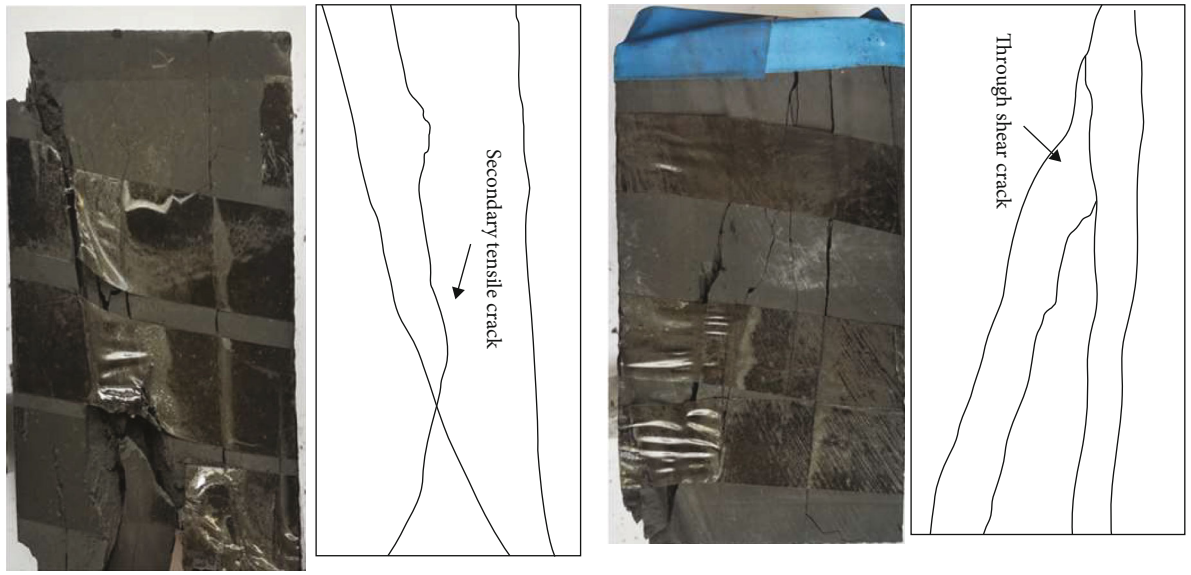

(e) $f = 3$ Hz, $p = 5$ MPa (f) $f = 9$ Hz, $p = 5$ MPa

Figure 4: Shale creep macroscopic fracture morphology.

function of axial pressure σ_1, seepage pressure p, disturbance frequency f, and creep time t, which is

$$D = F(\sigma_1, f, p, t). \tag{1}$$

The results of the perturbation creep test show that during the creep process, the creep damage variable D of the rock increases with time in the form of a negative exponential function. Therefore, this paper simplifies the damage variable D to formula (2)

$$D = 1 - \sigma_1^{-\alpha(p,f)t}. \tag{2}$$

In the formula, α is the disturbance factor, which is a function of the disturbance frequency f and the osmotic pressure p.

3.2. Establishment of Perturbation Creep Damage Model of Shale under Osmotic Pressure. After analyzing the results of uniaxial perturbation creep test of rock under osmotic pressure, it is found that the perturbed creep process of rock has the following characteristics:

(1) The creep curve of the rock will have an instantaneous sudden change at the moment when the axial load is applied, that is, the initial strain

(2) After the initial strain of shale, the creep rate of shale decreases, and the creep curve has an obvious decay process

(3) Both the seepage pressure and the disturbance load affect the axial stress value of the rock entering the accelerated creep stage. With the increase of disturbance frequency and seepage water pressure, the axial stress value of shale entering the accelerated creep stage decreases

Therefore, the model must include elastic elements, viscous elements, and viscoplastic elements. Because the rock has plasticity and a certain degree of initial damage, this article puts the plastic element in parallel with the damage element introduced in this article to form a plastic damage element. In recent years, the theory of fractional calculus has become a popular tool in studying the viscoelasticity of materials. It is widely used to describe the time memory effect and can describe the nonlinear changes of materials well. Therefore, this paper uses fractional calculus to establish a shale perturbation creep damage model under osmotic pressure on the basis of rock creep theory. Aiming at the creep characteristics of rock, this paper connects the modified fractional Maxwell body, the fractional nonlinear viscoplastic body (NAVPB body), and the plastic damage elements introduced in this article in series to form a modified nonlinear viscoelastic plastic damage creep model. The schematic diagram of the model is shown in Figure 5.

In the figure, η is the viscosity coefficient of the NAVPB body, E_1, E_2, ξ_1 is the material parameter, γ_i is the number of derivation, n is the creep index, t_F is the start time node of the creep disturbance, and σ_S is the yield limit of the material. D is the damage variable in the plastic damage component.

(1) When $\sigma + \Delta\sigma < \sigma_b, t < t_F$, only the fractional Maxwell body works in the model, thus:

$$\begin{aligned} \sigma &= \sigma_1 = \sigma_2, \\ \varepsilon &= \varepsilon_1 + \varepsilon_2. \end{aligned} \tag{3}$$

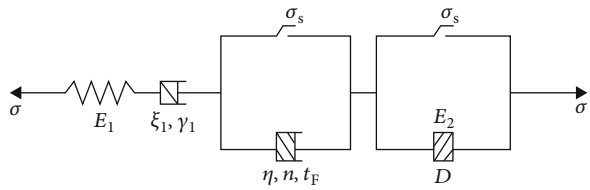

Figure 5: Creep damage model of shale.

In the above formula,

$$\begin{cases} \sigma_1 = E_1 \varepsilon_1, \\ \sigma_2 = \xi_1 \dfrac{\mathrm{d}^{\gamma_1} \varepsilon_2}{\mathrm{d}t^{\gamma_1}}. \end{cases} \tag{4}$$

Substituting (4) for Laplace transform and Laplace inverse transform into formula (3), the nonlinear rheological constitutive equation at $\sigma < \sigma_s$ can be obtained as follows:

$$\varepsilon = \frac{\sigma}{E_1} + {}_0D_t^{-\gamma_1}\left(\frac{\sigma}{\xi_1}\right). \tag{5}$$

In the formula, $D(\cdot)$ is the Riemann-Liouville type fractional calculus operator. Substituting the initial conditions $t = 0$ and $\sigma = \sigma_0$ into equation (5), the nonlinear creep equation can be obtained as follows:

$$\varepsilon = \frac{\sigma}{E_1} + \frac{\sigma}{\xi_1}\frac{t^{\gamma_1}}{\Gamma(1+\gamma_1)}, (0 < \gamma_1 < 1). \tag{6}$$

(2) When $\sigma_b < \sigma + \Delta\sigma < \sigma_a, t_b < t_F < t$, the damage element in the model works; the equation is

$$\varepsilon = \frac{\sigma}{E_1} + \frac{\sigma}{\xi_1}\frac{t^{\gamma_1}}{\Gamma(1+\gamma_1)} + \frac{\sigma}{E_2}(1\text{-}D), (0 < \gamma_1 < 1). \tag{7}$$

(3) When $\sigma + \Delta\sigma > \sigma_a, t_F > t$, NAVPB body starts to work in the model, and the equation is

$$\varepsilon = \frac{\sigma}{E_1} + \frac{\sigma}{\xi_1}\frac{t^{\gamma_1}}{\Gamma(1+\gamma_1)} + \frac{\sigma}{E_2}(1\text{-}D) + K\frac{\sigma - \sigma_a}{\eta}H(t - t_F), (0 < \gamma_1 < 1), \tag{8}$$

where ε is the longitudinal linear strain, σ_b is the proportional limit of the compressive strength of the rock, σ_a is the stress perturbation threshold of the NAVPB body, η is the viscosity coefficient of the NAVPB body, E_1, E_2, ξ_1 is the material parameter, γ_1 is the number of derivative calculations, and $K = F(\sigma, \Delta\sigma, p, f)$ is generally measured by experiment. t_b is the time node at which the rock reaches the limit of its compressive strength range.

3.3. The Influence of Different Factors on Damage Variables. After analyzing the model and test results, it is found that the damage variable D is a function of the axial pressure σ_l, the disturbance frequency f, the seepage pressure p, and the time t. The disturbance factor α is a function of the disturbance frequency f and the seepage water pressure p. This paper analyzes the influence of axial pressure σ_l, osmotic water pressure p, disturbance frequency f, and time t on the damage variable D to determine the functional formula of the damage variable.

3.3.1. Variation Law of Damage Variable D with σ_l, α, and t. Figure 6 shows the relationship curve between the damage variable D and the time t when the disturbance factor α and the axial pressure σ_l take different values. It can be seen from the figure that regardless of the value of the disturbance factor and the axial pressure, the damage variable D has basically the same trend over time, increasing with the increase of time, and the growth rate gradually decays and tends to stabilize. The difference is that the impact of axial compression on rock damage is more obvious at the initial stage of application, while the impact of disturbance factors on rock damage is slightly delayed in time. Changing the axial pressure, the change trend of the damage variable D with the disturbance factor E when $t = 120$ min is shown in Figure 6(b). Changing the disturbance factor, the change trend of damage variable D with axial pressure when $t = 120$ min is shown in Figure 6(c). The analysis shows that when $t = 120$ min, the influence of disturbance factor on damage variable D is more obvious.

3.3.2. The Change Law of Damage Variable D under the Action of f and p

(1) The Law of Influence of f and p on α. Draw the creep curve of shale under different disturbance and different seepage pressure conditions, and get the relation table of seepage water pressure, disturbance frequency, and disturbance factor. The values of the disturbance frequency, osmotic water pressure, and disturbance factor of each specimen obtained in the drawing are shown in Table 2.

In order to analyze the law of the effect of osmotic water pressure p and disturbance frequency f on the disturbance factor α, the relationship diagrams and disturbances between the disturbance frequency and the disturbance factor under the osmotic pressure of 1, 3, 5, 7, and 9 MPa are made using equation (2). The relationship between osmotic water pressure and disturbance factor at frequencies of 2, 4, 6, 8, and 10 Hz is shown in Figure 7.

Analysis of Figure 7 shows that when the osmotic pressure increases, the disturbance factor gradually increases, but the growth rate gradually slows down. As the disturbance frequency increases, the disturbance factor increases at a lower growth rate, and the growth rate also gradually slows down. When the disturbance frequency is close to 8 Hz, the growth rate of the disturbance factor is close to zero. This shows that the disturbance frequency and osmotic pressure have the same influence on the disturbance factor,

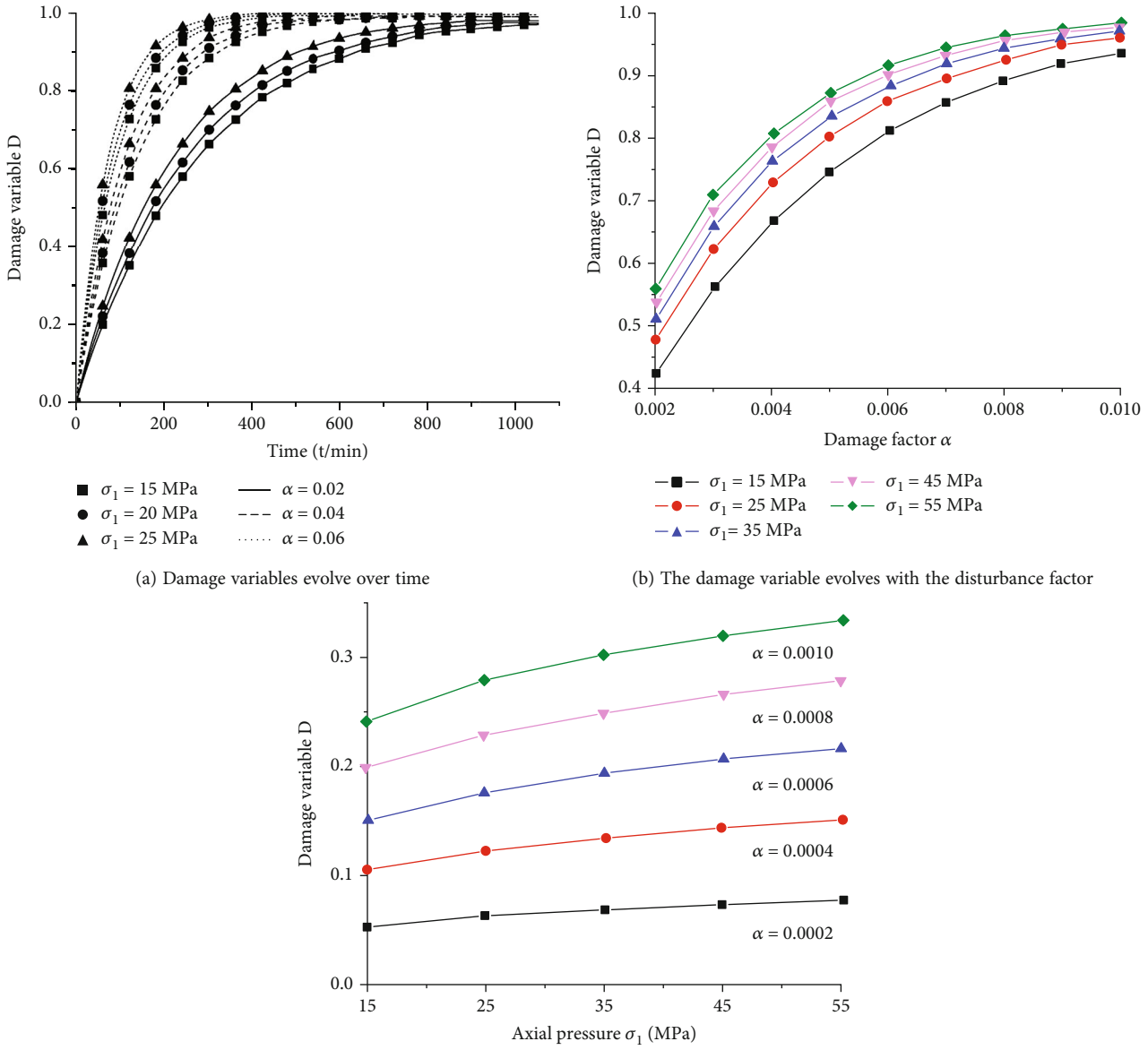

(a) Damage variables evolve over time

(b) The damage variable evolves with the disturbance factor

(c) The damage variable evolves with axial compression

Figure 6: The relation curve between D and σ_i, α, and t.

Table 2: Disturbance factor.

Serial number	Osmotic pressure p/MPa	Disturbance frequency f/Hz	α ($\times 10^{-4}$)
D1	0	0	0
D2	3	6	4.1312
D3	5	6	5.2813
D4	7	6	6.3298
D5	5	3	4.5099
D6	5	9	5.7683

but the degree of influence is different. The change trend of the disturbance factor α when the seepage water pressure increases is more obvious than when the disturbance frequency increases, which indicates that the rock damage is more sensitive to the seepage water pressure.

(2) The Law of Influence of f and p on D. In order to further obtain the influence of seepage water pressure and disturbance frequency on rock damage, according to the expression of the damage variable, plot the axial pressure σ_1=15, 25, 35 MPa and the damage variable D with the osmotic pressure when the time is 120 min (disturbance frequency is 6 Hz). The relationship between the change and the damage variable D with the disturbance frequency (the seepage pressure is 5 MPa) is shown in Figure 8.

Analysis of Figure 8 shows that when the axial pressure and the loading time are the same, as the osmotic pressure and the disturbance frequency increase, the damage variable

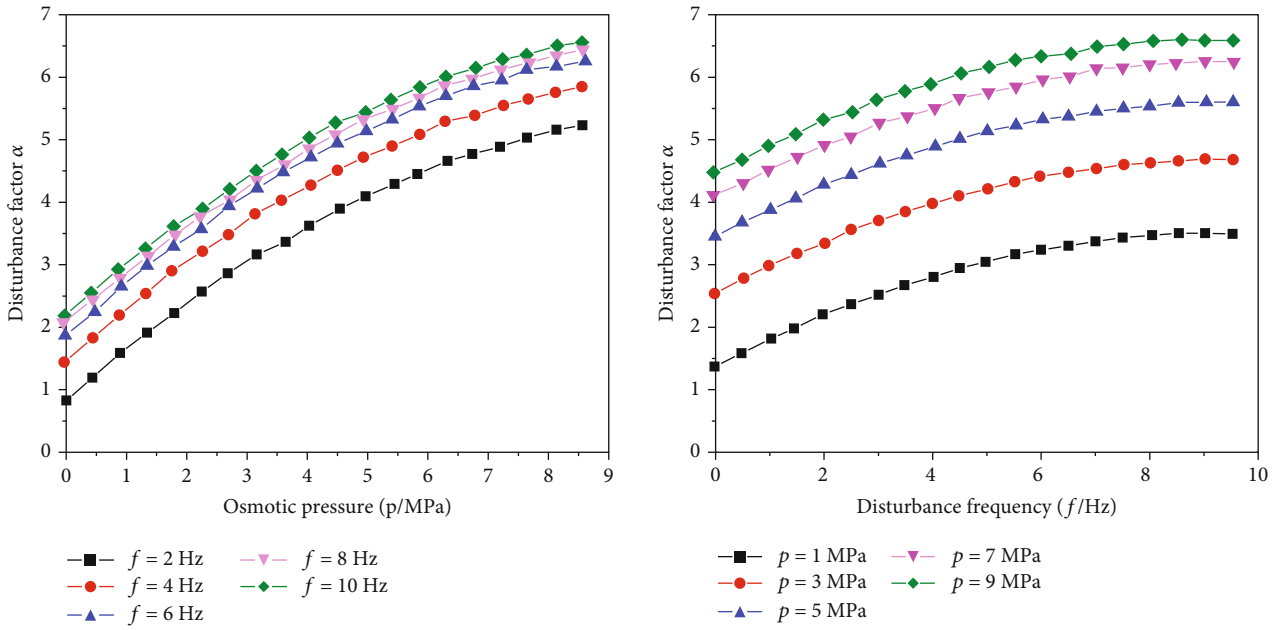

(a) Relationship between disturbance factor and osmotic pressure

(b) The relationship between disturbance factor and disturbance frequency

Figure 7: The influence of p and f on the disturbance factor α.

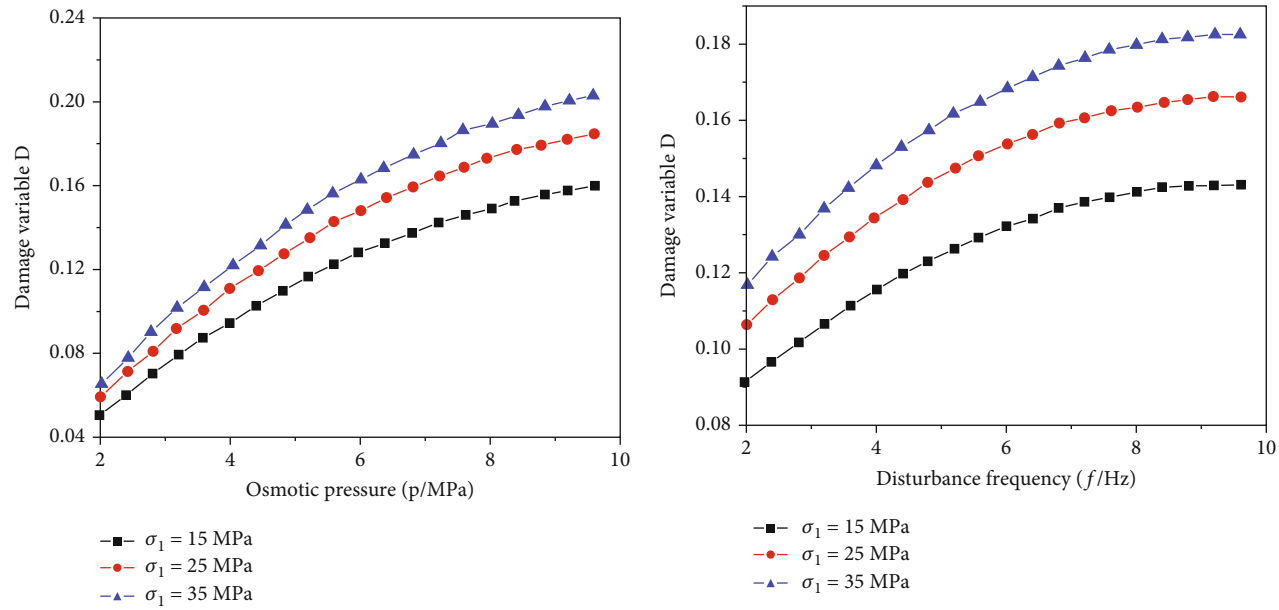

(a) Damage variable changes with osmotic pressure

(b) Damage variable changes with disturbance frequency

Figure 8: The influence of p and f on the damage variable D.

also increases, and it increases in a nonlinear manner. When the time is $t = 120$ min, the disturbance frequency is $f = 6$ Hz, and the axial pressure is 15, 25, and 35 MPa; the damage variables increase by 0.10898, 0.12601, and 0.13803 as the seepage water pressure increases. When the time is $t = 120$ min, the seepage water pressure is 5 MPa, and the axial pressure is 15, 25, and 35 MPa; as the disturbance frequency increases, the damage variables increase by 0.051998, 0.060101, and 0.064796, respectively. When the disturbance frequency is greater than 8 Hz, the damage variable gradually stabilizes, which further shows that rock damage is more sensitive to seepage pressure.

3.4. Perturbation Creep Damage Model of Shale under Osmotic Pressure Must Participate in the Verification. Through experiments and analysis, this paper chooses an

Table 3: Fitting results of shale creep damage model parameters under osmotic pressure.

Specimen number	σ_1/MPa	E_1/MPa	ξ_1/GPa·min	E_2/MPa	η/GPa·min	σ_s/MPa	t_F/min	n	α ($\times 10^{-4}$)	R^2
D2	15	22.998	76.406	588.012	56.988	23.52	1324	1.656	5.143	0.939
	25	18.403	85.992	567.024	36.828					
	35	22.986	88.825	545.993	25.511					
	45	25.897	85.306	571.792	19.464					
D5	15	22.293	76.322	567.846	56.156	23.12	1294	1.812	5.595	0.929
	25	17.534	81.954	549.535	33.222					
	35	20.996	79.012	582.994	21.292					
	45	23.350	72.698	596.989	13.895					

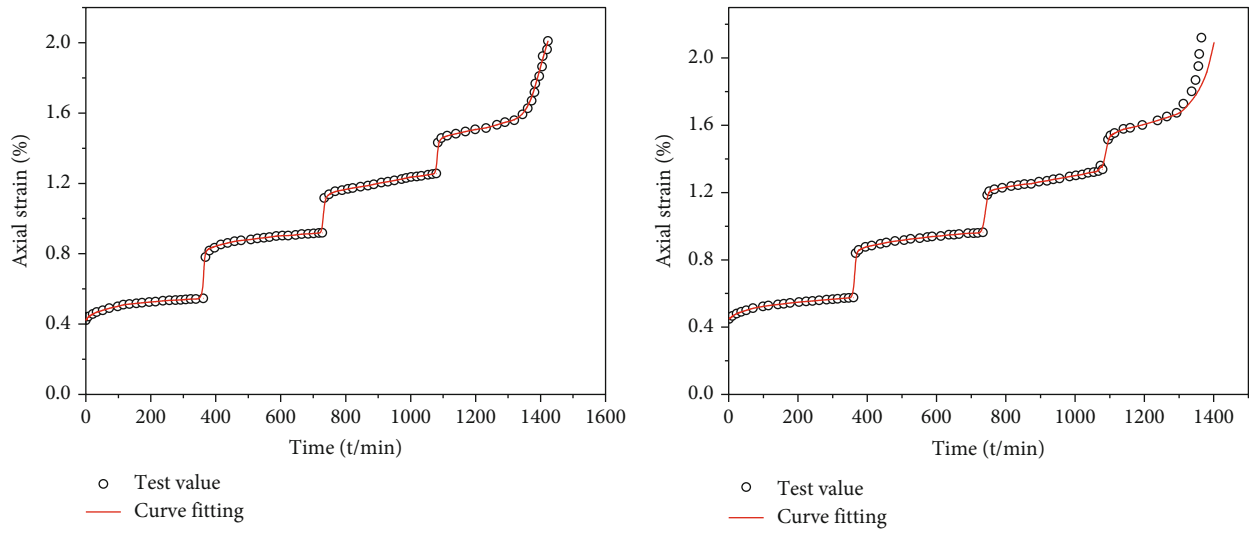

(a) $f = 6$ Hz, $p = 3$ MPa (b) $f = 3$ Hz, $p = 5$ MPa

Figure 9: Time-strain curve fitting diagram of rock creep.

improved nonlinear least squares method based on pattern search (PS) [19] to fit the data to determine the parameters of the perturbed creep damage model under osmotic pressure. The nonlinear least squares method based on pattern search is to make the algorithm find the best direction in the best direction that can optimize the target value by alternately detecting movement and pattern movement. The improved nonlinear least squares method based on pattern search is through the introduction of swarm intelligence algorithm the idea to improve the optimization effect [20]. The creep parameters of the model obtained by fitting are shown in Table 3. It can be seen from Figure 9 that the error of the predicted value is low, which fully illustrates the rationality and accuracy of the model.

4. Conclusion

(1) The disturbance load promotes the creep damage and fracture of the rock. When the perturbation frequency increases, the time from the beginning of creep to complete failure of the rock decreases, and the total strain of the rock increases. As the seepage pressure increases, the creep characteristics of shale are more sensitive to disturbance loads

(2) The application of disturbance load and osmotic pressure changes the creep failure mode of shale. When disturbance is applied, the way of shale failure becomes complicated. The increase of the disturbance frequency leads to an increase in the frequency of fracture opening and closing of shale and a slight increase in the number of cracks; the increase in seepage pressure leads to more complicated rock fracture modes. When the osmotic pressure increases, the failure mode of the rock transitions from the joint failure of tension and shear to the failure dominated by tension failure. The creep characteristics of rock are more significantly affected by osmotic pressure than by disturbance frequency

(3) In this paper, the perturbation creep damage model of rock under osmotic pressure considering seepage water pressure and perturbation frequency is established through experiment and theoretical analysis. In this paper, an improved nonlinear least squares

method based on pattern search (PS) is used to determine the parameters of the model, and the model is used for prediction. The error of the prediction results is very small

Data Availability

The data that support the findings of this study are obtained through experiments by the corresponding author and other authors. The data are true and reliable. All authors are willing to provide experimental data, and all data are available from the corresponding author.

Conflicts of Interest

The authors declare no competing interests.

Acknowledgments

This work was supported by the National Key Research and Development Program (2016YFC0600704), the Disciplinary Innovation Team of Liaoning Technical University (LNTU20TD-11), the National Natural Science Foundation of China (51404130), and the Natural Science Foundation of Liaoning Province (20180550708), and thanks are due to supports from Institute of Mechanics and Engineering of Liaoning Technical University.

References

[1] L. Xiaozhao, Q. Chengzhi, and S. Zhushan, "Meso-macro mechanical constitutive model under high seepage pressure in brittle rocks," *Chinese Journal of Rock Mechanics and Engineering*, vol. 39, 1, pp. 2593–2601, 2020.

[2] X. Wu, L. Changwu, S. Rongxi, and X. Yang, "Creep model of rock subjected to water pressure and external force," *Journal of Southwest Jiaotong University*, vol. 42, no. 6, pp. 720–725, 2007.

[3] W. Laigui, Z. Na, H. Feng, and L. Xin, "Rock creep damage model and its stability analysis," *Journal of China Coal Society*, vol. 34, no. 1, pp. 64–68, 2009.

[4] W. A. Junguang, L. Bing, and T. I. Mi, "Study of creep characteristics produced by nonlinear damage of oil shale in hydrous state," *Journal of experimental mechanics*, vol. 29, pp. 112–118, 2014.

[5] L. W. Chen, S. J. Li, Y. F. Chen, K. X. Zhang, and Y. X. Liu, "Further development and application of a creep damage model for water-bearing rocks," *Chinese Journal of Solid Mechanics*, vol. 39, no. 6, pp. 642–651, 2018.

[6] C. Yajun, W. Wei, and X. Weiya, "Permeability evolution of low-permeability rocks in triaxial creep tests," *Chinese Journal of Rock Mechanics and Engineering*, vol. 34, no. S2, pp. 3822–3829, 2015.

[7] S. Chengxue and C. Xuan, "Influence of high pore water pressure on creep properties of rock," *Chinese Journal of Rock Mechanics and Engineering*, vol. 29, no. 8, pp. 1603–1609, 2010.

[8] F. Zhiliang, *Theoretical and Experimental Study on Rock Creep Disturbance Effect and Damage Characteristics*, Shandong University of Science and Technology, Tai'an, 2007.

[9] Y. F. Gao, H. Q. Xiao, B. Wang, and Y. P. Zhang, "A rheological test of sandstone with perturbation effect and its constitutive relationship study," *Chinese Journal of Rock Mechanics and Engineering*, vol. 27, no. 1, pp. 3180–3185, 2008.

[10] B. Wang, Y. Gao, and J. Wang, "Evolution law analysis on surrounding rock stress field by rheology disturbed effects," *Journal of China Coal Society*, vol. 38, no. 9, pp. 1446–1450, 2010.

[11] X. Cui, J. Li, X. Niu, and S. Wang, "Experimental study on rheological regularity and constitutive relationship of rock under disturbing loads," *Chinese Journal of Rock Mechanics and Engineering*, vol. 26, no. 9, pp. 1875–1881, 2007.

[12] G. S. Su, L. H. Hu, X. T. Feng, J. H. Wang, and X. H. Zhang, "True triaxial experimental study of rock burst process under low frequency cyclic disturbance load combined with static load," *Chinese Journal of Rock Mechanics and Engineering*, vol. 35, no. 7, pp. 1309–1322, 2016.

[13] N. Jianguo and Z. Zhu, "Constitutive model of frozen soil with damage and numerical simulation of coupled problem," *Chinese Journal of Theoretical and Applied Mechanics*, vol. 39, no. 1, pp. 70–76, 2007.

[14] W. Qi-Hu, Y. Yi-Cheng, L. Yang-Zhang, and Y. Nan, "A creep constitutive model of rock considering initial damage and creep damage," *Rock and Soil Mechanics*, vol. 36, no. 1, pp. 57–62, 2016.

[15] O. M'Barki, S. Brame, O. Castellanos Diaz et al., "The effect of rock composition and microstructure on steam foam rheology in sandstone reservoirs," *Fuel*, vol. 287, p. 119471, 2021.

[16] M. Souley, F. Homand, S. Pepa, and D. Hoxha, "Damage-induced permeability changes in granite: a case example at the URL in Canada," *International Journal of Rock Mechanics and Mining Sciences*, vol. 38, no. 2, pp. 297–310, 2001.

[17] G. N. Boukharov, M. W. Chanda, and N. G. Boukharov, "The three processes of brittle crystalline rock creep," *International Journal of Rock Mechanics and Mining Sciences and Geomechanics Abstracts*, vol. 32, no. 4, pp. 325–335, 1995.

[18] M. Kachanov, "Effective elastic properties of cracked solids: critical review of some basic concepts," *Applied Mechanics Review*, vol. 45, no. 8, pp. 304–335, 1992.

[19] Z. Haining, "Photovoltaic cell parameter identification based on nonlinear least squares method," *Modern Electric Power*, vol. 34, no. 6, pp. 79–84, 2017.

[20] L. G. Li, Z. H. Zhang, Y. S. Dai, W. F. Sun, and C. Q. Dong, "Optimization of natural gas pipeline network operation based on improved pattern search algorithm," *Journal of China University of Petroleum (Edition of Natural Science)*, vol. 36, no. 4, pp. 139–143, 2012.